

Electronic Supporting Information (ESI) for the manuscript:

**Fine-tuning of the confined space in microporous metal-organic frameworks for
efficient mercury removal**

Marta Mon, Xiaoni Qu, Jesús Ferrando-Soria,* Isaac Pellicer-Carreño, Antonio
Sepúlveda-Escribano, Enrique V. Ramos-Fernandez, Johannes C. Jansen, Donatella
Armentano* and Emilio Pardo*

Experimental Section

Chemicals

All chemicals were of reagent grade quality. They were purchased from commercial sources and used as received. Compound $(\text{Me}_4\text{N})_2\{\text{Cu}_2[(\text{S,S})\text{-methiomox}](\text{OH})_2\} \cdot 4\text{H}_2\text{O}$ was prepared as reported earlier.¹

Preparation of $\{\text{Cu}^{\text{II}}_4[(\text{S,S})\text{-methox}]_2\} \cdot 5\text{H}_2\text{O}$ (**1**).

2.0 g (2.75 mmol) of $(\text{Me}_4\text{N})_2\{\text{Cu}_2[(\text{S,S})\text{-methiomox}](\text{OH})_2\} \cdot 4\text{H}_2\text{O}$ were dissolved in 20 mL of H_2O . To the resulting dark green solution, another aqueous acid solution (HCl, pH = 3) was added slowly, under a continuous stirring, to reach a final pH value of *ca.* 5.5. The green polycrystalline solid that appeared was filtered off, washed with water and methanol and dried under vacuum. Yield: 1.25 g, 87%; Anal.: calcd for $\text{C}_{24}\text{Cu}_4\text{H}_{42}\text{S}_4\text{N}_4\text{O}_{17}$ (1041.1): C, 27.69; H, 4.07; S, 12.32; N, 5.38%. Found: C, 27.39; H, 3.89; S, 12.39; N, 5.51%. IR (KBr): $\nu = 3021, 2968 \text{ cm}^{-1}$ (C-H), 1613 cm^{-1} (C=O).

Alternatively, well-shaped hexagonal prisms of **1** suitable for X-ray structural analysis were obtained by layering 2 mL of a pH = 2.5 aqueous solution over *ca.* 15 mL of another aqueous solution of $(\text{Me}_4\text{N})_2\{\text{Cu}_2[(\text{S,S})\text{-methiomox}](\text{OH})_2\} \cdot 4\text{H}_2\text{O}$ (0.15 gr) in an essay tube. After two weeks of slow diffusion, the crystals were isolated by filtration on paper and air-dried. Anal.: calcd for $\text{C}_{24}\text{Cu}_4\text{H}_{42}\text{S}_4\text{N}_4\text{O}_{17}$ (1041.1): C, 27.69; H, 4.07; S, 12.32; N, 5.38%. Found: C, 27.48; H, 3.95; S, 12.29; N, 5.42%. IR (KBr): $\nu = 3021, 2973 \text{ cm}^{-1}$ (C-H), 1611 cm^{-1} (C=O).

Syntheses of $(\text{HgCl}_2)_{0.5}@[\text{Cu}^{\text{II}}_4[(\text{S,S})\text{-methox}]_2] \cdot 3\text{H}_2\text{O}$ (**0.5HgCl₂@1**) and $\text{HgCl}_2@[\text{Cu}^{\text{II}}_2[(\text{S,S})\text{-methox}]_2] \cdot 2\text{H}_2\text{O}$ (**HgCl₂@1**).

Well-formed hexagonal green prisms of **0.5HgCl₂@1** and **HgCl₂@1**, which were suitable for X-ray diffraction, were obtained by soaking crystals of **1** (5.0 mg) in a saturated $\text{H}_2\text{O}/\text{CH}_3\text{OH}$ (1:1) solution of HgCl_2 for 24 and 336 hours, respectively. The crystals were washed with water, isolated by filtration on paper and air-dried. **0.5HgCl₂@1**: Anal.: calcd for $\text{C}_{24}\text{ClCu}_4\text{H}_{38}\text{Hg}_{0.5}\text{S}_4\text{N}_4\text{O}_{15}$ (1140.8): C, 25.27; H, 3.36; S, 11.24; N, 4.91%. Found: C, 25.11; H, 3.21; S, 11.27; N, 4.92%. IR (KBr): $\nu = 1613 \text{ cm}^{-1}$ (C=O). **HgCl₂@1**: Anal.: calcd for $\text{C}_{24}\text{Cl}_2\text{Cu}_4\text{H}_{34}\text{HgS}_4\text{N}_4\text{O}_{14}$ (1256.5): C, 22.91; H, 2.88; S, 10.19; N, 4.45%. Found: C, 22.97; H, 2.61; S, 10.21; N, 4.43%. IR (KBr): $\nu = 1609 \text{ cm}^{-1}$ (C=O).

¹ M. Mon, J. Ferrando-Soria, T. Grancha, F. R. Fortea-Pérez, J. Gascon, A. Leyva-Pérez, D. Armentano, E. Pardo, *J. Am. Chem. Soc.* **2016**, *138*, 7864–7867.

Experiments with mixtures of metal salts in solution

Uptake capacity and kinetic profile of 1: Firstly, the maximum uptake capacity of compound **1** as well as the speed of the adsorption HgCl₂ process were analysed. For that, *ca.* 100 mg of **1** were soaked in a water/methanol (1:1) saturated solution of HgCl₂. A few milligrams were taken at different lapse intervals during two weeks (Fig. S1 and Table S2), washed with water and analysed by ICP-MS.

Ion selectivity tests: We evaluated the selectivity of **1** towards HgCl₂ in the presence of other metal cations usually present in drinking water [Na^I, Mg^{II}, Ca^{II}, Al^{III} and Fe^{III}] together with the speed of the adsorption process, by soaking 100 mg of polycrystalline powder of **1** in an aqueous solution containing equimolar amounts (2 mmol) of HgCl₂, NaCl, MgCl₂, CaCl₂, AlCl₃ and FeCl₃ for 72 hours. A few milligrams were taken at different lapse intervals (Fig. 2b and Table S3), washed with water and analyzed by ICP-MS, which indicated that only the mercury salts were adsorbed by **1** in all cases with a similar kinetic profile of that observed in the absence of these metal cations (Fig. S1).

Kinetic profile of the water cleaning process: In order to evaluate the kinetics and the efficiency of the capture process, 50 mg of a polycrystalline sample of **1** were soaked in 10 mL of an aqueous solution containing HgCl₂ (10 ppm, pH \approx 7.0). The mixture was stirred at room temperature and 200 μ L aliquots were extracted at different time intervals (see text and Fig. 2c and Table S4), the ion concentration being estimated through ICP-MS analyses.

Physical Techniques

Elemental (C, H, N), and ICP-MS analyses were performed at the Microanalytical Service of the Universitat de València. FT-IR spectra were recorded on a Perkin-Elmer 882 spectrophotometer as KBr pellets. The thermogravimetric analysis was performed on crystalline samples under a dry N₂ atmosphere with a Mettler Toledo TGA/STDA 851° thermobalance operating at a heating rate of 10 °C min⁻¹.

Gas adsorption: The N₂ and CO₂ adsorption-desorption isotherms at 77, 273 and 298 K (Fig. S12), were carried out on a polycrystalline sample of **1** with a Micromeritics ASAP2020 instrument. Sample was first activated with methanol and then evacuated at 348 K during 19 hours under 10⁻⁶ Torr prior to their analysis.

The N₂ adsorption isotherm at 77 K on **1** (a) indicates a very low surface area. In fact, the value obtained after application of the BET model is 8 m²/g, and the pore volume calculated with the Dubinin-Radushkevich (DR) equation is also very small (0.01 cc/g) and is far below the crystallographic one.

These values indicate that N₂ cannot penetrate into the pores of the solid. Regarding the CO₂ adsorption isotherm at 273 K, it can be seen that there is a CO₂ uptake comparable to that of others MOFs at these conditions (SIM-1,² ZIF-8,³ etc). After application of the DR method to the CO₂ adsorption data at 273 K, the pore volume value of this material is 0.11 cc/g.

Finally, we have measured the adsorption of CO₂ and N₂ at 298 K, in order to assess if accessibility of the nitrogen molecule is also limited at room temperature. No N₂ adsorption at room temperature was observed, whereas CO₂ is effectively adsorbed (Fig. S12). This is a good indication that these two molecules can be separated by material **1**. However, the separation can only be checked by breakthrough experiments (see below).

Breakthrough measurements: Breakthrough curve experiments for different mixtures of gases were carried out using a column at 298 K (Fig. S13). The sample powder was packed in the middle part of the column. Here, the sample mass we used is 0.30 g. Breakthrough allows in situ activation of the sample under Helium flow. Mass flow controllers controlled the flow rates of all gases. Before the measurement, the sample was activated at the desired temperature for 19 hours. The gas stream from the outlet of the column was analysed online with a mass spectrometer. The preparation of a fixed bed for breakthrough experiments is not a trivial point. When activated carbons or zeolites are used for breakthrough, the powders are pelletized, in order to get and controlled particle size and furthermore the bed is compressed. In this way it is possible to achieve a quasi-plug flow or piston flow through the column. In the case of MOF the difficulties to prepare pellets or the stability issues that many MOFs present upon compression, limits the degree of freedom to prepare fixed beds that allows a quasi-piston flow through the bed. For that reason we used inert gas (H₂) that allows us to track the deviation of the flow from the ideal flow. The amount of gas adsorbed was the difference between the shape of the CH₄, N₂ and CO₂ breakthrough and the H₂ breakthrough. Thus, the dispersion and the very small pressure drop can be considered.

The N₂/CO₂ separation is fully achieved with compound **1**. As we can see, N₂ breaks at the same time that H₂ does, indicating that N₂ is not adsorbed at all. However CO₂ is adsorbed during 250 seconds. It shows that selectivity for this separation is infinite. Considering that N₂ is fed in excess, this result is very relevant. This notorious result encouraged us to try other difficult separations. For CH₄/CO₂ we can see that the separation performance is also exceptional (infinite). If we quantified the amount of CO₂ adsorbed in both breakthrough experiments. We can see that the adsorption capacity is ~4.7 cc/g. This capacity is

² S. Aguado, C.-H. Nicolas, V. Moizan-Basle, Carlos Nieto, Hedi Amrouche, Nicolas Bats, N. Audebrand, D. Farrusseng, *New J.Chem.*, **2011**, 35, 41–44.

³ B. A. Russell, A. D. Migone, *Microporous and Mesoporous Materials*, **2017**, 246, 178–185.

the same that the one found in the adsorption isotherm (~5 cc/g at 158 torr the partial pressure used in the breakthrough experiments). It indicates that compound **1** only adsorbs CO₂ and the material reach the maximum capacity for CO₂.

X-ray crystallographic data collection and structure refinement: Crystals of **1**, **0.5HgCl₂@1** and **HgCl₂@1** with *ca.* 0.16 x 0.18 x 0.20, 0.20 x 0.22 x 0.22 and 0.08 x 0.12 x 0.12 mm as dimensions were selected and mounted on a MITIGEN holder in Paratone oil and very quickly placed on a liquid helium (**1** and **HgCl₂@1**) or nitrogen (**0.5HgCl₂@1**) stream cooled at 45 (**1** and **HgCl₂@1**) and 90 K (**0.5HgCl₂@1**) to avoid the possible degradation upon dehydration. Diffraction data for **1** and **HgCl₂@1** were collected using synchrotron at CRYSTAL (**1**) and I19 (**HgCl₂@1**) beamlines of the SOLEIL and DIAMOND at $\lambda = 0.67165$ and 0.6889 Å, respectively, whereas on a Bruker-Nonius X8APEXII CCD area detector diffractometer using graphite-monochromated Mo-K α radiation ($\lambda = 0.71073$ Å) for **0.5HgCl₂@1**. The data were processed through CrysAlisPro⁴ (**1**), SAINT⁵ reduction and SADABS⁶ multi-scan absorption (**0.5HgCl₂@1**) and xia2⁷ (**HgCl₂@1**) software. The structure was solved with the SHELXS structure solution program, using the Patterson method. The model was refined with version 2013/4 of SHELXL against F^2 on all data by full-matrix least squares.⁸

Crystals of **0.5HgCl₂@1** and **HgCl₂@1**, suitable for X-ray diffraction, were obtained by soaking crystals of **1** (5.0 mg) in a saturated H₂O/CH₃OH (1:1) solution of HgCl₂ for 24 hours and two weeks respectively, after a crystal-to-crystal transformation. For these reasons it is reasonable to observe a diffraction pattern sometimes affected by expected internal imperfections of the crystals (likely at the origin of some Alert level A for **0.5HgCl₂@1** in checkcif related to complex anisotropic displacement parameters in the main residue for some C, N and O atoms of the ligand and in **HgCl₂@1** for larger than expected residual density maximum on metal atom location). Marked deficiencies as ruptures within the single crystal appeared after soaking, this might generate a false twinning situation and is likely at the origin of larger than expected positive residual density on copper metal ions, detected as levels Alert A in checkcif of **HgCl₂@1**.

In all samples, all non-hydrogen were refined anisotropically except disordered oxygen from water molecules [O2W and O3W] and Cl atoms in **0.5HgCl₂@1**. In **HgCl₂@1** crystal structure Hg(1) atom is

⁴ CrysAlisPro 1.171.38.41 (Rigaku Oxford Diffraction, 2015).

⁵ SAINT, version 6.45, Bruker Analytical X-ray Systems, Madison, WI, 2003.

⁶ Sheldrick G.M. J. Appl.Cryst. 48 (2015) 3-10

⁷ (a) Evans, P. (2006) Acta Cryst. D62, 72-82; (b) Evans, P. R. and Murshudov, G. N. (2013) Acta Cryst. D69, 1204-1214; (c) Winn, M. D. et al. (2011) Acta Cryst. D67, 235-242; (d) Winter, G. (2010) J. Appl. Cryst. 43, 186-190.

⁸ (a) G. M. Sheldrick, Acta Cryst. A71 (2015) 3-8. (b) G. M. Sheldrick, Acta Cryst. 2008, A64, 112-122.

statistically disordered on two positions imposed by symmetry [symmetry code: 1-x, 1-y, z; see also in Fig.S3 HgCl₂ molecules in the bigger pores). The occupancy factors, of HgCl₂ molecules have been defined accordingly with SEM results. The use of some C-C and C-S together with Hg-Cl (in **0.5HgCl₂@1**) bond lengths restrains during the refinements of some highly disordered atoms even for Hg(1)-Cl in **0.5HgCl₂@1**, has been reasonable imposed and related to ethylenethiomethyl chains of the methox ligand and terminal chloride atoms that are dynamic components of the frameworks.

In **HgCl₂@1**, the supposed Hg₂ imposed by symmetry (i: 1- y, x, - 0.5 + z) it is not really present, in agreement with assigned occupancy factor (0.25 instead of the imposed 0.5). Consequently the C7···Hg2I of 1.55 Å is not reliable.

The solvent molecules were disordered but, even if not all the ones detected by TGA analysis, have been somehow modelled (Alert level B for **1**, related to mismatch in the ratio of given/expected molecular weight). For that reason, in **0.5HgCl₂@1**, the contribution to the diffraction pattern from the diffuse electron density located in the voids was subtracted from the observed data through the SQUEEZE method, implemented in PLATON.⁹ The hydrogen atoms of the ligand in all three structure refinement were set in calculated positions and refined as riding atoms whereas for water molecules were neither found nor calculated.

A summary of the crystallographic data and structure refinement for the three compounds is given in Table S1. The somewhat high R values (levels Alert A and B in checkcif) in **0.5HgCl₂@1** is, most likely, affected, as stated above, by internal imperfections of the crystals and by the contribution of the disordered solvent to the intensities of the low angle reflections. CCDC 1558088-1558090 for **1**, **0.5HgCl₂@1** and **HgCl₂@1**, respectively.

The final geometrical calculations on free voids and the graphical manipulations were carried out with PLATON⁷ implemented in WinGX,¹⁰ and CRYSTAL MAKER¹¹ programs, respectively.

⁹ (a) Spek, A. L. *Acta Crystallogr. Sect. C-Struct. Chem.* **2015**, 71, 9-18. (b) Spek, A. L. *Acta Crystallogr. Sect. D, Biol. Crystallogr.* **2009**, 65, 148.

¹⁰ Farrugia, L. J. *J. Appl. Crystallogr.* **1999**, 32, 837.

¹¹ D. Palmer, CRYSTAL MAKER, Cambridge University Technical Services, C. No Title, 1996.

Table S1. Summary of Crystallographic Data for **1**, **0.5HgCl₂@1** and **HgCl₂@1**.

Compound	1	0.5HgCl₂@1	HgCl₂@1
Formula	C ₂₄ H ₄ Cu ₄ N ₄ O ₁₇ S ₄	C ₂₄ H ₃₈ ClCu ₄ Hg _{0.50} N ₄ O ₁₅ S ₄	C ₂₄ H ₃₄ Cl ₂ Cu ₄ HgN ₄ O ₁₄ S ₄
<i>M</i> (g mol ⁻¹)	1041.01	1140.73	1256.44
λ (Å)	0.67165	0.71073	0.6889
Crystal system	tetragonal	tetragonal	tetragonal
Space group	<i>P</i> 4 ₂	<i>P</i> 4 ₂	<i>P</i> 4 ₂
<i>a</i> (Å)	13.6593(2)	13.0954(15)	12.9735(2)
<i>c</i> (Å)	12.0051(4)	11.5653(13)	11.5283(3)
<i>V</i> (Å ³)	2239.88(10)	1983.3(5)	1940.35(8)
<i>Z</i>	2	2	2
ρ_{calc} (g cm ⁻³)	1.544	1.910	2.151
μ (mm ⁻¹)	1.751	4.386	5.805
<i>T</i> (K)	45	90	45
θ range for data collection (°)	1.49- 24.69	1.56- 24.99	1.521- 28.00
Completeness to $\theta = 25.0$	100%	100%	100%
Measured reflections	20924	25429	29039
Unique reflections (Rint)	3630	3494	5164
Observed reflections [<i>I</i> > 2 σ (<i>I</i>)]	2936	2914	4754
Goof	0.957	1.043	0.999
Absolute structure parameter (Flack)	0.02(4)	0.18(5)	0.030(7)
<i>R</i> ^a [<i>I</i> > 2 σ (<i>I</i>)] (all data)	0.0516 (0.0696)	0.1045 (0.1177)	0.0799 (0.0831)
<i>wR</i> ^b [<i>I</i> > 2 σ (<i>I</i>)] (all data)	0.1215 (0.1329)	0.2617 (0.2708)	0.2319 (0.2370)

^a $R = \sum(|F_o| - |F_c|) / \sum |F_o|$. ^b $wR = [\sum w(|F_o| - |F_c|)^2 / \sum w|F_o|^2]^{1/2}$.

Table S2. Adsorption data^a from the ICP-MS analyses for the HgCl₂ adsorption by **1**.

Time (min.)	HgCl ₂ adsorption
0	0.0000
1	10.230
5	12.750
10	14.330
15	14.340
20	14.280
25	14.270
30	14.320
35	14.310
40	14.340
45	14.290
50	14.280
55	14.260
60	14.290
300	14.670
720	15.020
1440	16.090
2880	18.130
4320	20.370
5760	23.160
8640	24.260
11520	26.670
14400	28.430
17280	28.610
20160	28.430

^a HgCl₂ adsorption (wt. %) extracted from the ICP-MS analyses.

Table S3. Selected data^a from the ICP-MS analyses for the HgCl₂, NaCl, MgCl₂, CaCl₂, AlCl₃ and FeCl₃ adsorption by **1**.

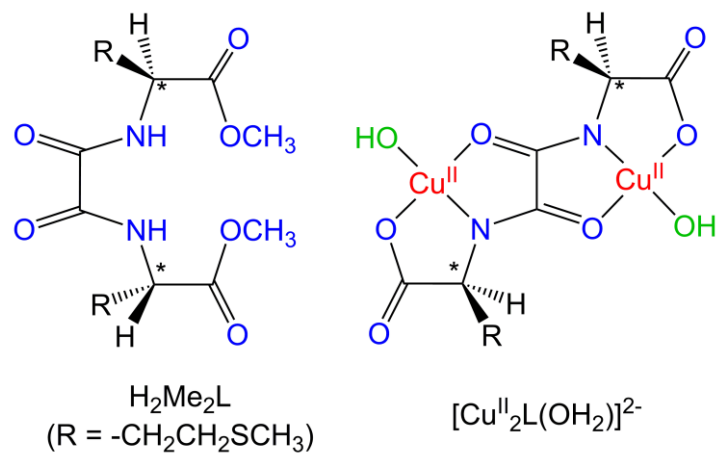
Time (min.)	<i>HgCl₂ adsorption</i>	<i>NaCl adsorption</i>	<i>MgCl₂ adsorption</i>	<i>CaCl₂ adsorption</i>	<i>AlCl₃ adsorption</i>	<i>FeCl₃ adsorption</i>
0	0.00	0.00	0.00	0.00	0.00	0.00
1	10.23	0.01	0.01	0.01	0.01	0.03
5	12.75	0.00	0.00	0.00	0.00	0.02
10	14.33	0.00	0.00	0.00	0.00	0.00
15	14.34	0.02	0.03	0.03	0.01	0.01
20	14.28	0.01	0.02	0.02	0.00	0.00
25	14.27	0.00	0.00	0.00	0.00	0.00
30	14.32	0.00	0.01	0.03	0.03	0.01
35	14.31	0.00	0.00	0.02	0.02	0.00
40	14.34	0.03	0.00	0.00	0.00	0.00
45	14.29	0.02	0.03	0.01	0.01	0.01
50	14.28	0.00	0.02	0.00	0.00	0.00
55	14.26	0.00	0.00	0.00	0.00	0.00
60	14.29	0.01	0.01	0.01	0.01	0.03
300	14.17	0.01	0.00	0.00	0.00	0.02
720	14.51	0.01	0.00	0.00	0.00	0.00
1440	14.77	0.00	0.01	0.01	0.01	0.03

^a Metal adsorption (wt. %) extracted from the ICP-MS analyses.

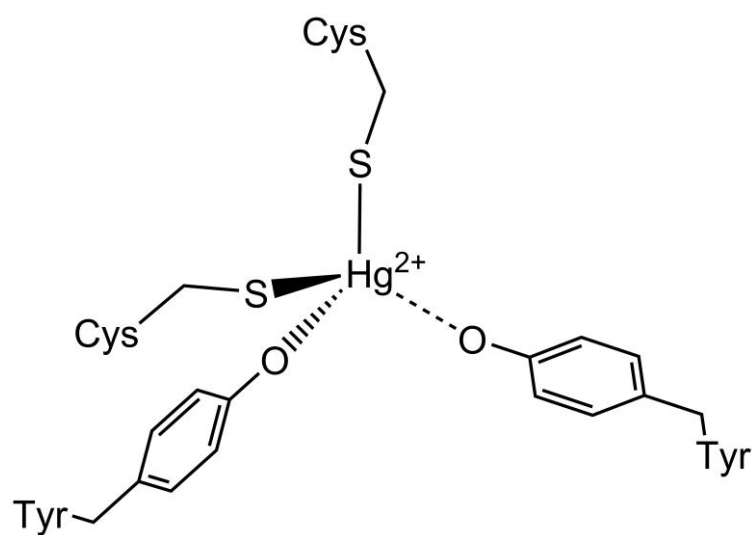
Table S4. Selected data^a from the ICP-MS analyses^b for the aqueous mother solution during the Hg²⁺ adsorption process^c by a polycrystalline sample of **1**.

Time (min.)	[Hg ²⁺]
0	10159
5	248.1
10	77.12
15	2.01
30	2.03
45	1.77
60	1.68
75	1.34
90	1.38
120	1.47
180	1.89
240	1.23
300	1.01
360	1.12
720	1.96
1440	1.13

^a Results are given as µg/L. ^b L.D.: 0,012 µg/L. ^c Cu was not detected by ICP analyses confirming the integrity of **1** in the adsorption process.



Scheme S1. Chemical structures of the chiral bis(amino acid)oxalamide ligand (left), highlighting the potential coordination sites and chiral centers and the corresponding dianionic bis(hydroxo) dicopper(II) complex (right).



Scheme S2. Schematic representation of the active site of the enzyme mercury reductase (MR).

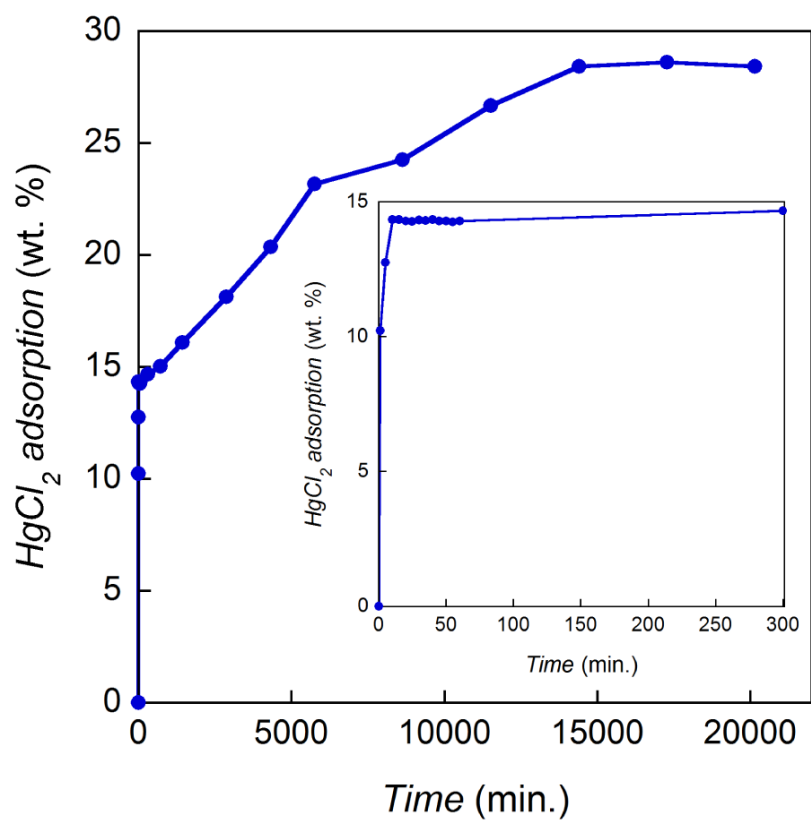


Fig. S1. HgCl₂ adsorption vs. time curve of **1** in a water/methanol (1:1) saturated solution of HgCl₂. The inset shows in detail the 0-300 min. range.

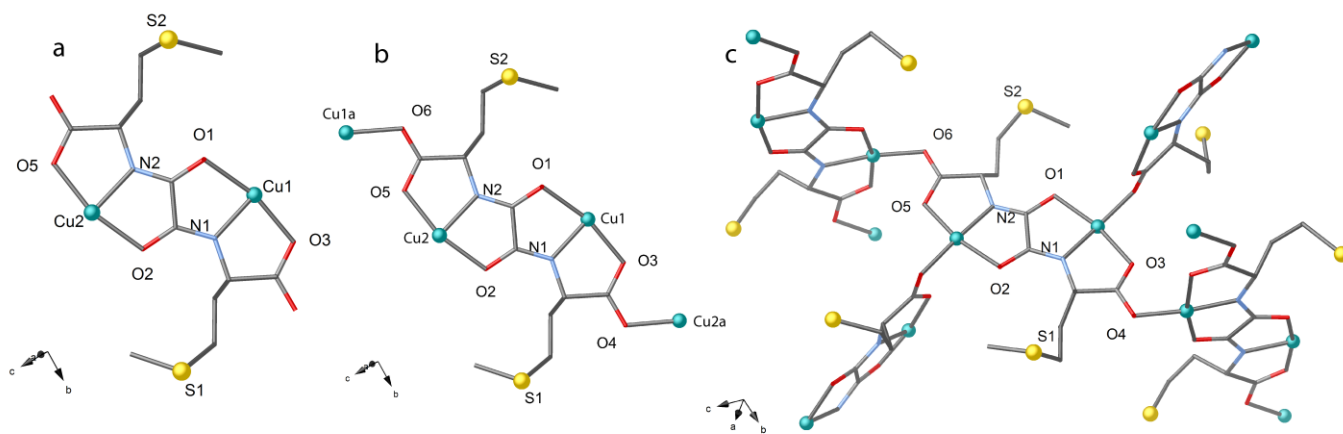


Fig. S2. Asymmetric unit of **1** consisting of *trans* oxamidato-bridged dicopper(II) units $\{\text{Cu}^{\text{II}}_2[(\text{S,S})\text{-methox}]\}$; (a) assembled each other through the carboxylate groups (b and c). Free water solvent molecules are omitted for clarity.

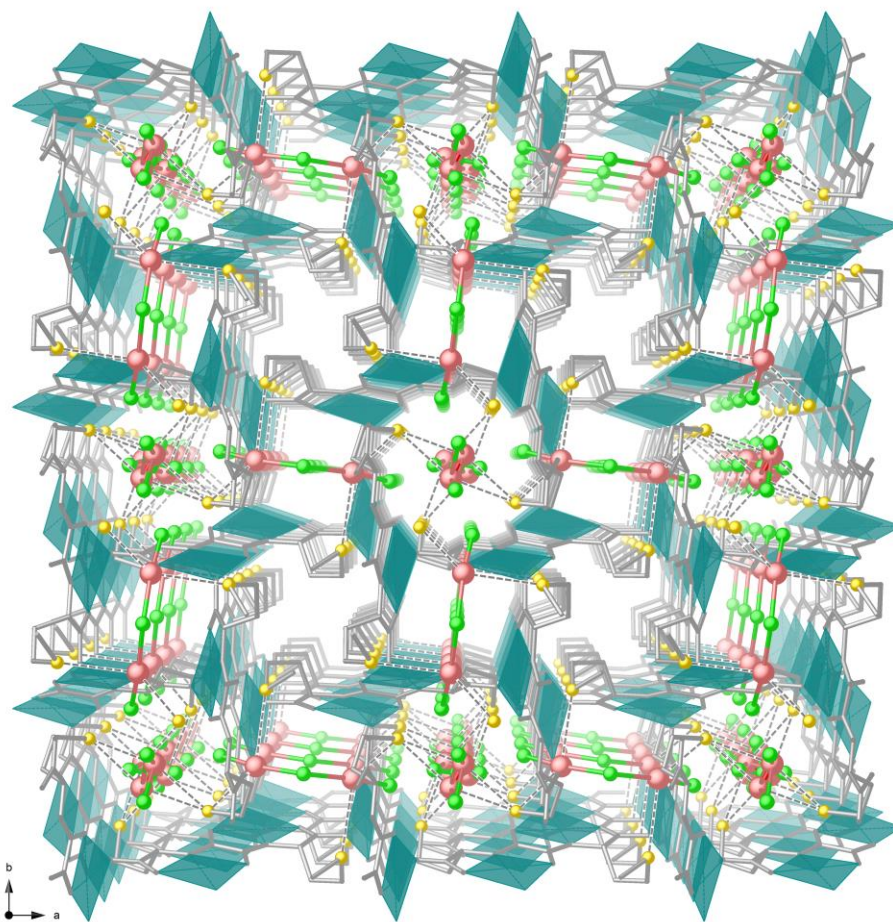


Fig. S3. Perspective view along the crystallographic *c* axis of the structure of **HgCl₂@1**. Copper atoms and ligands (except S atoms) forming the network are represented by cyan polyhedra and grey sticks, respectively. Mercury, chloride and sulphur atoms are depicted as pale pink, green and gold spheres. Free water solvent molecules are omitted for clarity.

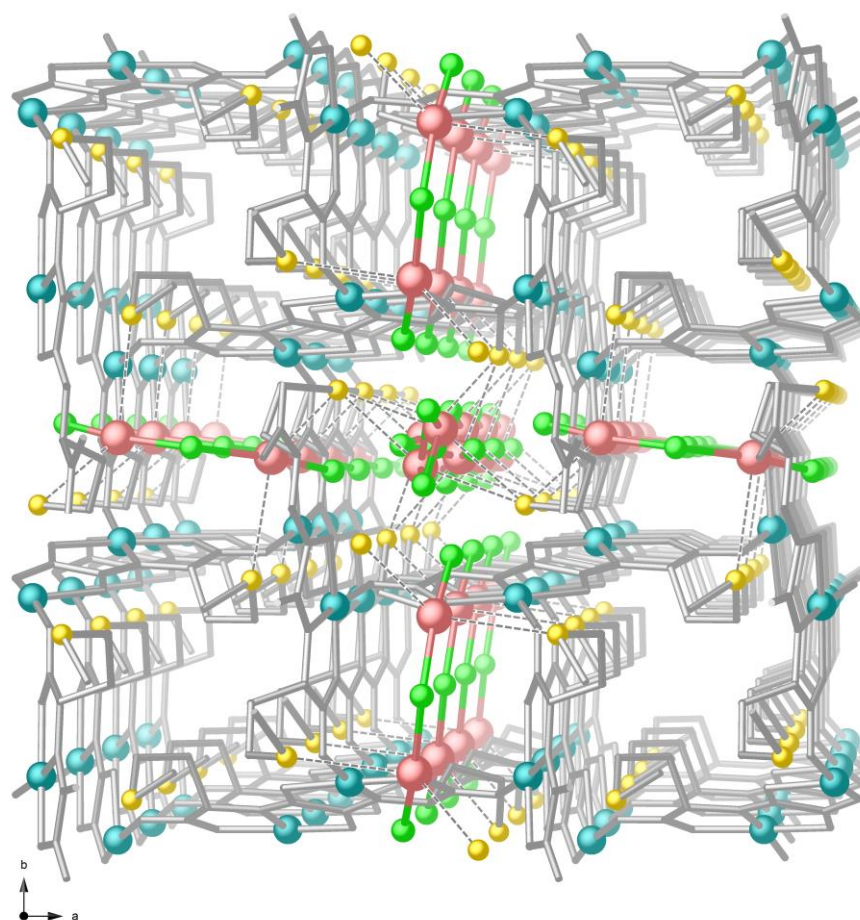


Fig. S4. Perspective view of a fragment of $\text{HgCl}_2@1$ along the c axis surrounded by the chloride-bridged dinuclear $[\text{Hg}_2(\mu\text{-Cl})\text{Cl}_3]$ entities, filling interstitial voids, close to medium size pores. Copper atoms and ligands (except S atoms) forming the network are represented by cyan polyhedra and grey sticks, respectively. Mercury, chloride and sulphur atoms are depicted as pale pink, green and gold spheres. Free water solvent molecules are omitted for clarity.

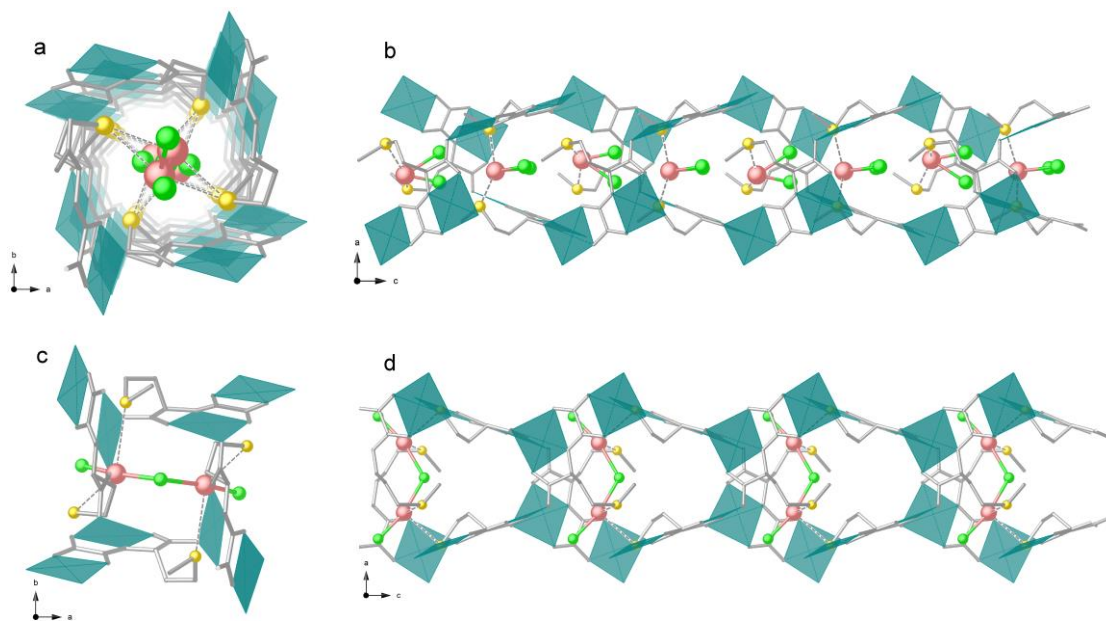


Fig. S5. Detailed view of one single channel of **HgCl₂@1** along the *c* axis (**a**) and side view (**b**). View along *c* axis (**c**) and lateral (**d**) of one channel of chloride-bridged dinuclear [Hg₂(μ-Cl)Cl₃] entities weakly interacting with thioether arms of the host matrix. Copper atoms and ligands (except S atoms) forming the network are represented by cyan polyhedra and grey sticks, respectively. Mercury, chloride and sulphur atoms are depicted as pale pink, green and gold spheres. Free water solvent molecules are omitted for clarity.

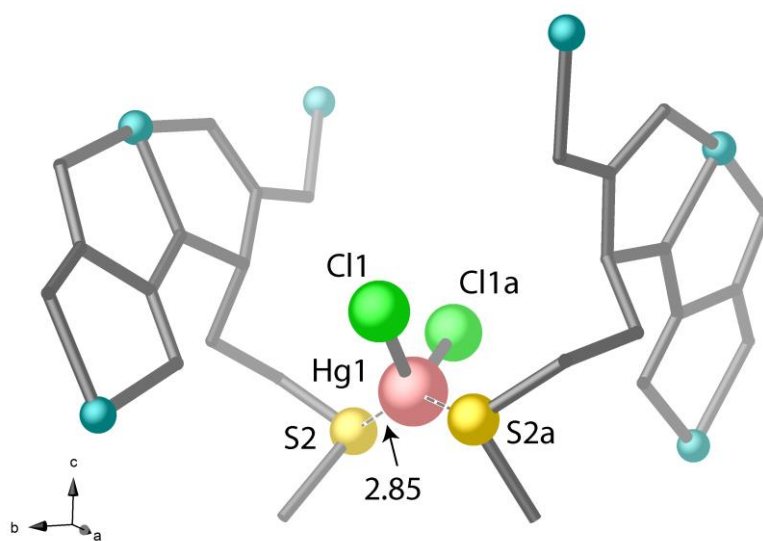


Fig. S6. Perspective views of a portion of **0.5HgCl₂@1** showing details of the interaction of HgCl₂ molecules with the MOF walls. Water solvent molecules are omitted for clarity. Bond lengths are reported in Å. Color scheme: Copper, Mercury, chloride and sulphur atoms are depicted as cyan, pale pink, green and gold spheres. Atoms and ligands (except S atoms) forming the network are represented by grey sticks. [Symmetry code (a): 2-x, -y, z].

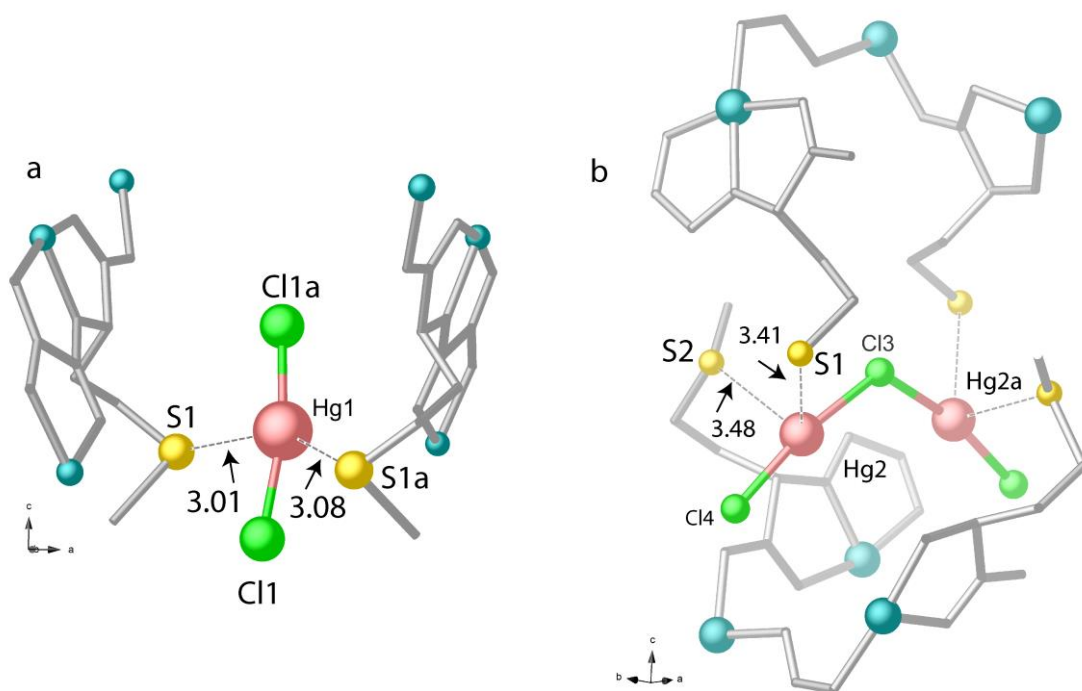


Fig. S7. Perspective views of a portion of $\text{HgCl}_2@1$ showing details of the interaction of not equivalent Hg1 (a) and Hg2 (b) for HgCl_2 and $[\text{Hg}_2(\mu\text{-Cl})\text{Cl}_3]$ moieties with the MOF walls. Bond lengths are reported in Å. Colour scheme: Copper, Mercury, chloride and sulphur atoms are depicted as cyan, pale pink, green and gold spheres. Atoms and ligands (except S atoms) forming the network are represented by grey sticks. [Symmetry code (a): $1-x, 1-y, z$]

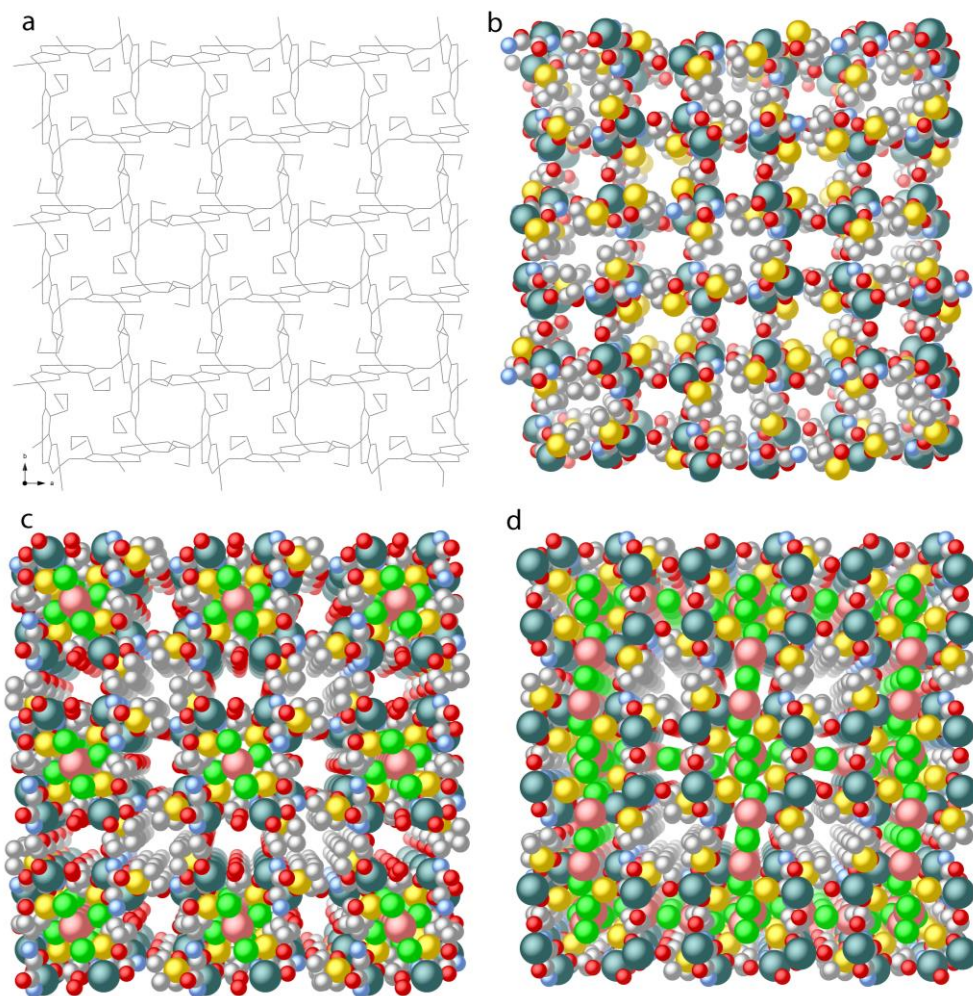


Fig. S8. Comparison of crystal structures of **1** represented as wireframe (**a**) or space-filling (**b**) models, with $0.5\text{HgCl}_2@1$ (**c**) and $\text{HgCl}_2@1$ (**d**) nets (in space filling model with Van der Waals radii showing adsorbed molecules). Copper, Mercury, chloride, sulphur, carbon, oxygen and nitrogen atoms are depicted as cyan, pale pink, green, gold, grey, red and pale blue spheres.

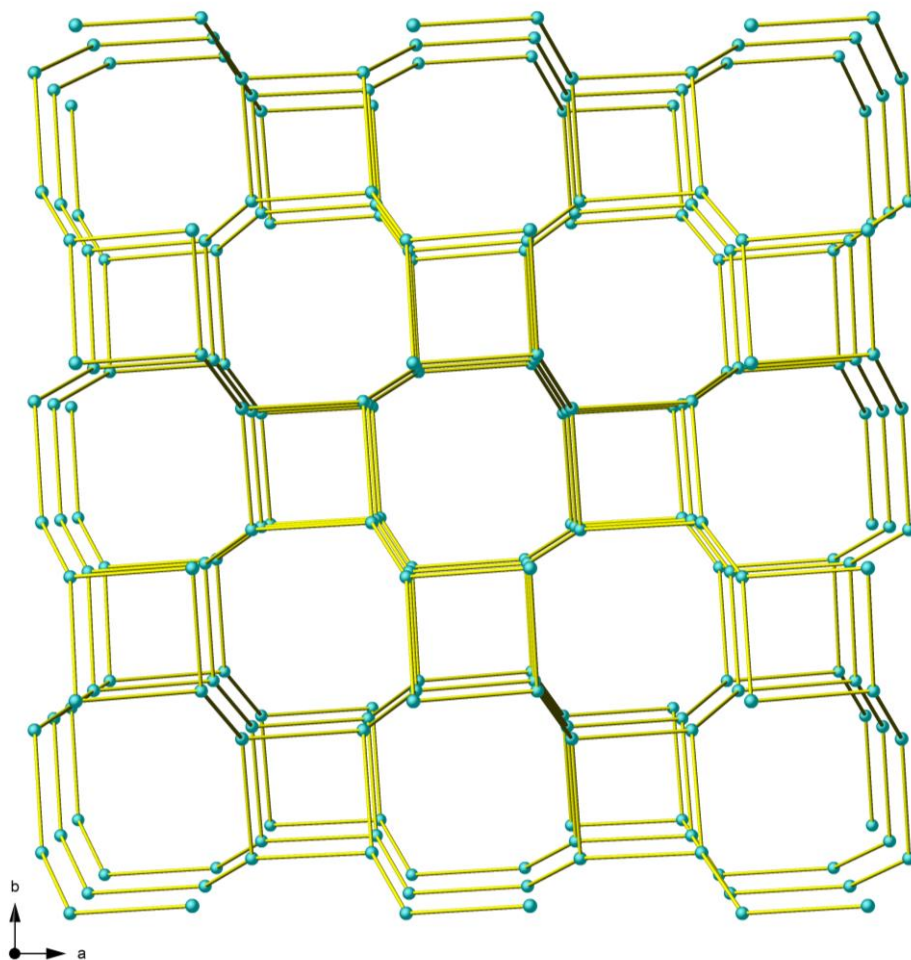


Fig. S9. The 3-c srs net in **1**.

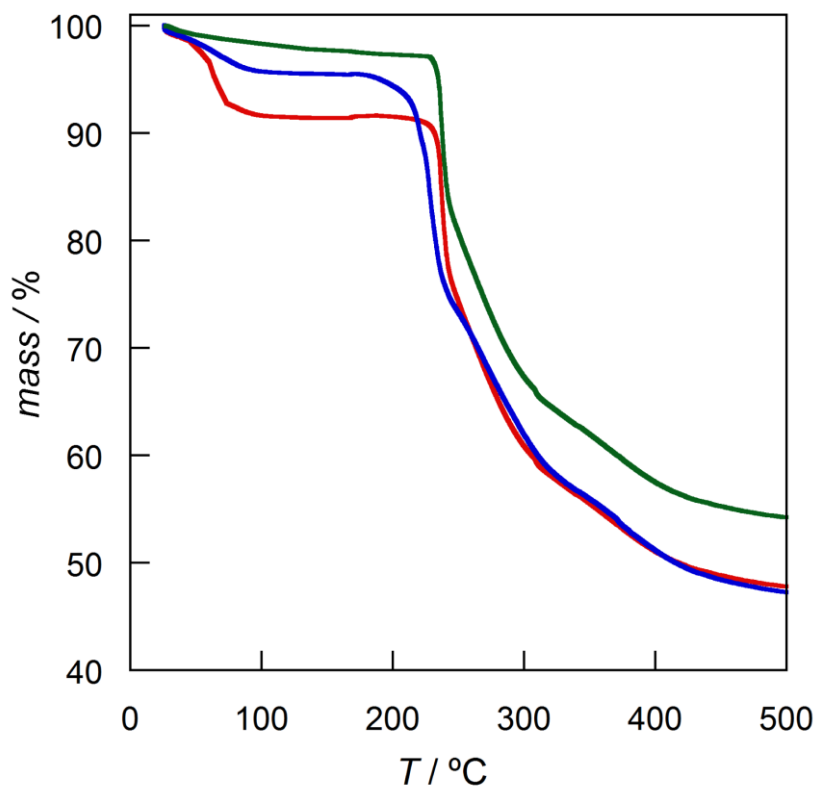


Fig. S10. Thermo-Gravimetric Analyses (TGA) of **1** (red), **0.5HgCl₂@1** (blue) and **HgCl₂@1** (green) under a dry N₂ atmosphere.

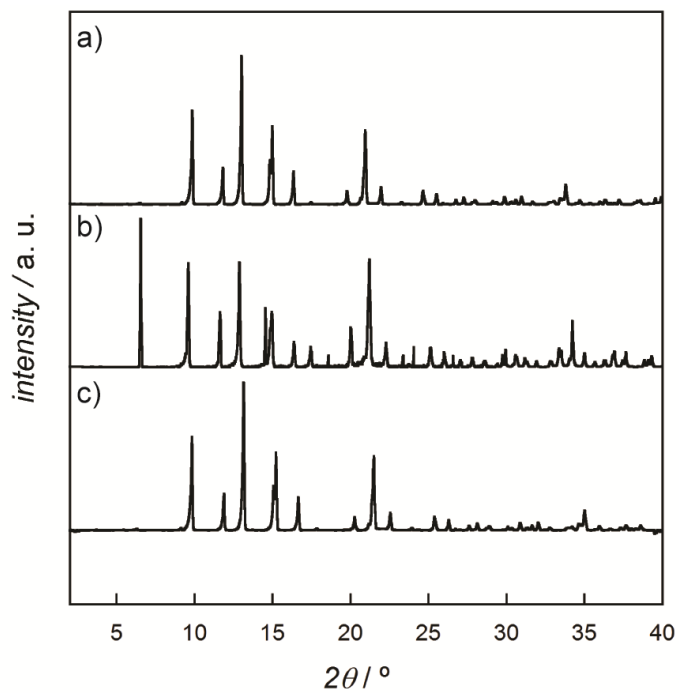


Fig. S11. Experimental PXRD pattern profile of **1** (a), **HgCl₂@1** (b) and **1'** (c, after the HgCl₂ extraction process) in the 2θ range 2–40°.

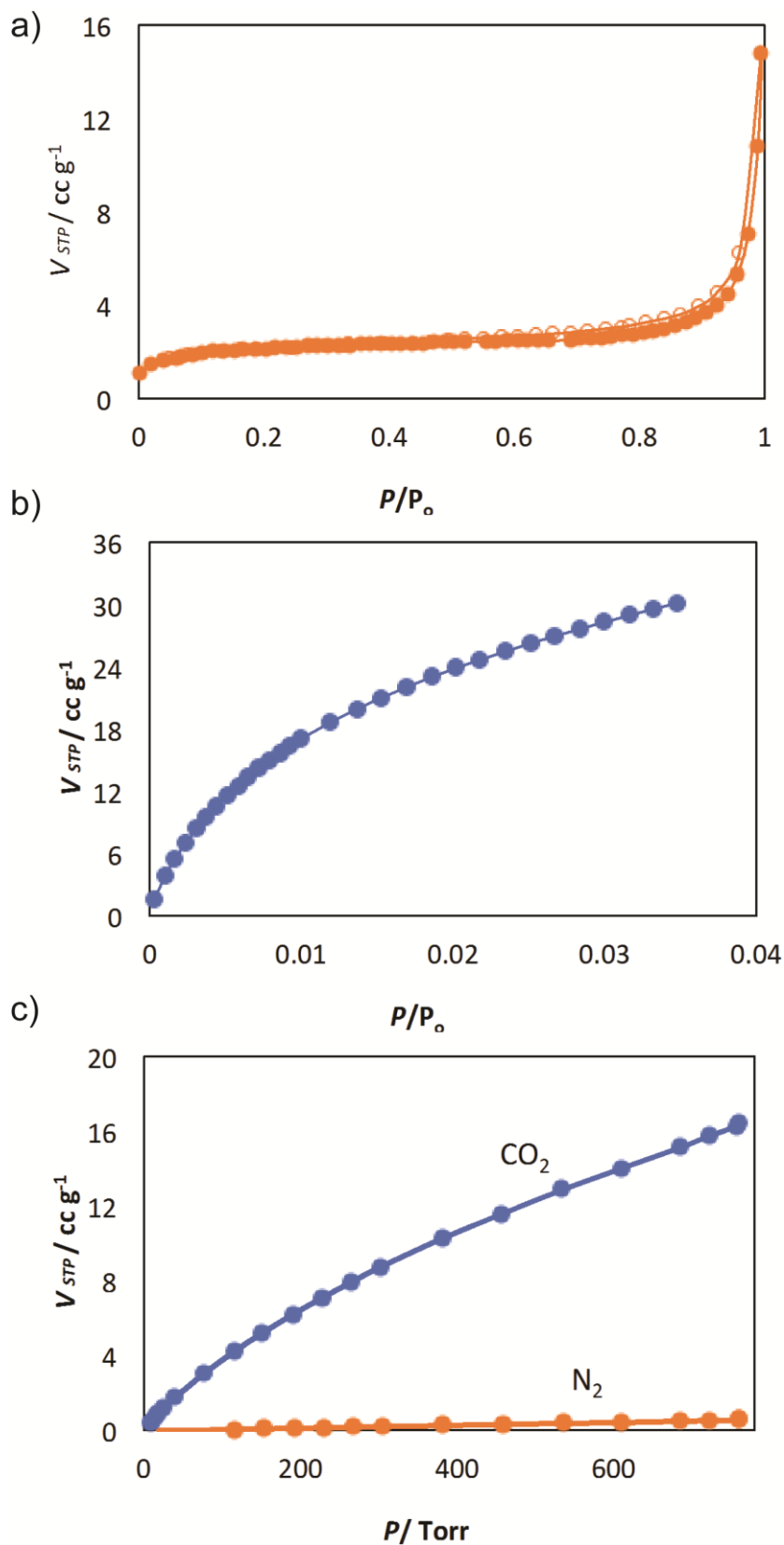


Fig. S12. N_2 (a) and CO_2 (b) sorption isotherms for the activated compound **1** at 77 and 273 K, respectively. c) N_2 and CO_2 sorption isotherms for **1** at 298 K.

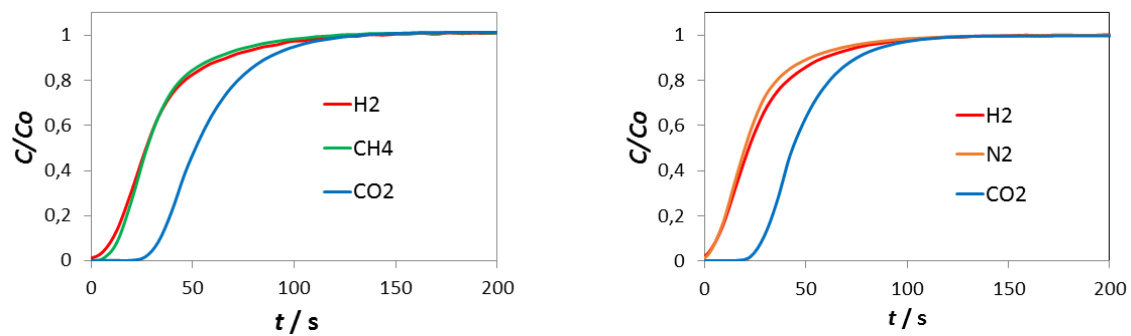


Fig. S13. Experimental column breakthrough curves for left CH₄/CO₂ and right N₂/CO₂ gas mixtures (75:25, v/v) measured at 298 K and 1 bar in a column using **1** as stationary phase. The total flow was 1.2 ml•min⁻¹. H₂ was used as reference gas.